The Plastidial 2-*C*-Methyl-D-Erythritol 4-Phosphate Pathway Provides the Isoprenyl Moiety for Protein Geranylgeranylation in Tobacco BY-2 Cells [C][W]

Esther Gerber,[a,1,2] Andréa Hemmerlin,[a,1] Michael Hartmann,[a] Dimitri Heintz,[a] Marie-Andrée Hartmann,[a] Jérôme Mutterer,[a] Manuel Rodríguez-Concepción,[b,3] Albert Boronat,[b] Alain Van Dorsselaer,[c] Michel Rohmer,[d] Dring N. Crowell,[e,4,5] and Thomas J. Bach[a,5]

[a] Institut de Biologie Moléculaire des Plantes (Centre National de la Recherche Scientifique, Unité Propre de Recherche 2357, associated with the Université Louis Pasteur), F-67083 Strasbourg, France

[b] Departament de Bioquímica i Biologia Molecular, Universitat de Barcelona, E-08028 Barcelona, Spain

[c] Université Louis Pasteur/Centre National de la Recherche Scientifique, Laboratoire de Spectrométrie de Masse Bio-Organique, Institut Pluridisciplinaire Hubert Curien, LC4-Unité Mixte de Recherche 7178, Ecole Européenne de Chimie, Polymères et Matériaux, F-67087 Strasbourg, France

[d] Université Louis Pasteur/Centre National de la Recherche Scientifique, Institut Le Bel, F-67070 Strasbourg, France

[e] Department of Biology, Indiana University–Purdue University, Indianapolis, Indiana 46202

Protein farnesylation and geranylgeranylation are important posttranslational modifications in eukaryotic cells. We visualized in transformed *Nicotiana tabacum* Bright Yellow-2 (BY-2) cells the geranylgeranylation and plasma membrane localization of GFP-BD-CVIL, which consists of green fluorescent protein (GFP) fused to the C-terminal polybasic domain (BD) and CVIL isoprenylation motif from the *Oryza sativa* calmodulin, CaM61. Treatment with fosmidomycin (Fos) or oxoclomazone (OC), inhibitors of the plastidial 2-*C*-methyl-D-erythritol 4-phosphate (MEP) pathway, caused mislocalization of the protein to the nucleus, whereas treatment with mevinolin, an inhibitor of the cytosolic mevalonate pathway, did not. The nuclear localization of GFP-BD-CVIL in the presence of MEP pathway inhibitors was completely reversed by all-*trans*-geranylgeraniol (GGol). Furthermore, 1-deoxy-D-xylulose (DX) reversed the effects of OC, but not Fos, consistent with the hypothesis that OC blocks 1-deoxy-D-xylulose 5-phosphate synthesis, whereas Fos inhibits its conversion to 2-*C*-methyl-D-erythritol 4-phosphate. By contrast, GGol and DX did not rescue the nuclear mislocalization of GFP-BD-CVIL in the presence of a protein geranylgeranyltransferase type 1 inhibitor. Thus, the MEP pathway has an essential role in geranylgeranyl diphosphate (GGPP) biosynthesis and protein geranylgeranylation in BY-2 cells. GFP-BD-CVIL is a versatile tool for identifying pharmaceuticals and herbicides that interfere either with GGPP biosynthesis or with protein geranylgeranylation.

INTRODUCTION

Protein isoprenylation refers to the covalent, thioether linkage of a C_{15} (farnesyl) or C_{20} (geranylgeranyl) group to a C-terminal Cys residue (Clarke, 1992; Zhang and Casey, 1996; Crowell, 2000). This modification mediates protein membrane and, in many cases, protein–protein interactions. In eukaryotes, protein farnesyltransferase (PFT) catalyzes the transfer of a farnesyl moiety from farnesyl diphosphate (FPP) to the Cys residue of a protein with a C-terminal CaaX motif (C = Cys; a = aliphatic; X = Met, Gln, Ala, Cys, or Ser). Protein geranylgeranyltransferase type 1 (PGGT 1) catalyzes the transfer of a geranylgeranyl moiety from geranylgeranyl diphosphate (GGPP) to the Cys residue of a protein with a similar C-terminal CaaX motif (X = Leu or Ile). PFT and PGGT 1 are cytosolic, heterodimeric metalloenzymes and consist of an identical α-subunit complexed to a unique β-subunit. A third protein isoprenyltransferase, RAB geranylgeranyltransferase, consists of unique α- and β-subunits and catalyzes the geranylgeranylation of RAB proteins bound to the RAB ESCORT PROTEIN (Crowell, 2000).

In plants, protein isoprenylation has been the subject of much study because of its fundamental role in phytohormone signaling and meristem development (Randall et al., 1993; Swiezewska et al., 1993; Cutler et al., 1996; Pei et al., 1998; Running et al., 1998, 2004; Bonetta et al., 2000; Yalovsky et al., 2000;

Ziegelhoffer et al., 2000). Both farnesylated and geranylgeranylated proteins are involved in abscisic acid (ABA) signaling. The existence of farnesylated negative regulators of ABA signaling is inferred from the ABA hypersensitive phenotype of ENHANCED RESPONSE TO ABA1 (*ERA1*) mutants of *Arabidopsis thaliana*, which lack the β-subunit of PFT (Cutler et al., 1996; Pei et al., 1998). In addition, two geranylgeranylated proteins, ROP2 and ROP6, have been shown to be involved in negative regulation of ABA signaling (Lemichez et al., 2001; Li et al., 2001; Yang, 2002). Similarly, the existence of geranylgeranylated proteins involved in negative regulation of auxin signaling is inferred from the enhanced response of GERANYLGERANYL TRANSFERASE β (*GGB*) mutants, which lack the β-subunit of PGGT 1, to auxin-induced lateral root initiation (Johnson et al., 2005). Mutants lacking either of two geranylgeranylated G protein γ-subunits were subsequently shown to exhibit the same phenotype (Trusov et al., 2007). The role of protein isoprenylation in meristem development is revealed by the phenotype of *Arabidopsis* mutants lacking either the β-subunit of PFT (*era1*) (Running et al., 1998; Bonetta et al., 2000; Yalovsky et al., 2000; Ziegelhoffer et al., 2000) or the shared α-subunit of PFT and PGGT 1 (*plp*) (Running et al., 2004). The former exhibits enlarged meristems and supernumerary floral organs, especially petals. The latter exhibits an exaggerated *era1-like* phenotype, suggesting that PGGT 1 compensates for loss of PFT in *era1* mutants. This suggestion was confirmed by suppression of the *era1* phenotype in *Arabidopsis* plants overproducing the PGGT 1 β-subunit (Johnson et al., 2005). Protein isoprenylation is also involved in plant stress responses. The isoprenylated molecular chaperone ANJ1 (a DnaJ protein homolog from *Atriplex nummularia*) is involved in protection from heat stress via regulation of protein folding (Zhu et al., 1993). In addition, isoprenylated heavy metal binding proteins confer tolerance to heavy metal stress (Dykema et al., 1999; Suzuki et al., 2002). Finally, protein isoprenylation is involved in regulation of the cell cycle. This was first shown using inhibitors of protein isoprenylation (Qian et al., 1996; Hemmerlin and Bach, 1998; Hemmerlin et al., 2000) and later supported by the observation that the farnesylated *Arabidopsis* nucleosome assembly protein (NAP1;1) regulates cell proliferation and expansion during different stages of leaf development (Galichet and Gruissem, 2006).

Despite the insights gained in recent years into the functions of farnesylated and geranylgeranylated plant proteins, the biosynthetic origins of the FPP and GGPP used by plant cells for protein isoprenylation have been controversial because, unlike yeast and animal cells, which rely exclusively on the cytosolic and putatively peroxisomal mevalonate (MVA) pathway (Kovacs et al., 2002), higher plants possess two distinct isoprenoid biosynthetic pathways: a cytosolic MVA pathway and a plastidial 2-*C*-methyl-D-erythritol 4-phosphate (MEP) pathway (cf. Rohmer, 1999; Lichtenthaler, 2000; Eisenreich et al., 2001, 2004; Rodríguez-Concepción and Boronat, 2002; Kuzuyama and Seto, 2003; Bouvier et al., 2005). In two independent studies, tobacco (*Nicotiana tabacum*) Bright Yellow-2 (BY-2) cells and spinach (*Spinacia oleracea*) seedlings were incubated with radiolabeled MVA, and labeling of proteins was observed (Randall et al., 1993; Shipton et al., 1995). Most of these proteins were found to be in the plasma membrane or nuclear/mitochondrial fractions. How-

ever, this observation does not prove that the MVA pathway is solely responsible for the biosynthesis of the isoprenyl diphosphates used by plant cells for protein isoprenylation. Indeed, incubation of BY-2 cells in the presence of $[2\text{-}^{14}C]1\text{-deoxy-}D\text{-}$xylulose (DX), the dephosphorylated form of the first product of the MEP pathway, resulted in significant labeling of low molecular weight proteins (Hemmerlin et al., 2003). The assumption that C_{15} and C_{30} isoprenoids are derived from the MVA pathway and C_5, C_{10}, C_{20}, and C_{40} isoprenoids are derived from the MEP pathway (cf. Rodríguez-Concepción and Boronat, 2002) suggests the possibility of a role for the MEP pathway in protein geranylgeranylation. However, this assumption cannot be entirely true because exchange of MVA and MEP pathway intermediates and products (i.e., crosstalk) has been demonstrated, although these interactions, for the most part, were demonstrated following elicitation of defense responses (Piel et al., 1998; Jux et al., 2001) or treatment with inhibitors (Kasahara et al., 2002; Hemmerlin et al., 2003; Laule et al., 2003). Other reasons also exist to question this assumption. For example, snapdragon (*Antirrhinum majus*) flowers produce both monoterpenoid (C_{10}) and sesquiterpenoid (C_{15}) volatiles that are derived from the MEP pathway (Dudareva et al., 2005). Thus, the extent to which transport of isoprenoid intermediates across the plastid envelope contributes to the biosynthesis of isoprenoid end products remains an open question. With this in mind, we extended our studies on isoprenoid crosstalk using transformed BY-2 cells expressing a geranylgeranylated green fluorescent protein (GFP), which is suited for both microscopy and biochemical studies. This approach was also used to develop a general reporter system for geranylgeranylation in situ and as a test system for inhibitors that interfere with protein geranylgeranylation directly, through inhibition of PGGT 1, or with geranylgeranyl diphosphate biosynthesis, through inhibition of the relevant isoprenoid biosynthetic pathway (or pathways) in plant cells. The geranylgeranylated GFP (GFP-BD-CVIL) used in this study was based on the rice (*Oryza sativa*) calmodulin CaM61 (Xiao et al., 1999; Dong et al., 2002), but only the C-terminal 45 amino acids of CaM61 were fused to GFP to avoid calcium binding and other physiological and/or regulatory functions that might influence protein localization (Boonburapong and Buaboocha, 2007). These 45 amino acids consist of a polybasic domain followed by a CVIL motif. Studies with the petunia (*Petunia hybrida*) calmodulin CaM53 (Rodríguez-Concepción et al., 1999), which bears a similar C-terminal polybasic domain followed by a CTIL geranylgeranylation motif, predicted that GFP-BD-CVIL would be geranylgeranylated and plasma membrane localized in BY-2 cells (Caldelari et al., 2001), whereas unprenylated GFP-BD-CVIL (i.e., in the presence of PGGT 1 or GGPP biosynthesis inhibitors) would be nuclear.

RESULTS

Cloning of the C-Terminal Moiety of Rice Calmodulin (CaM61) and Construction of GFP Fusion Proteins

We have shown that BY-2 cells are useful for studying regulatory interactions between isoprenoid biosynthesis and fundamental

processes like cell division and growth (Hemmerlin and Bach, 1998, 2000; Hemmerlin et al., 2000) and for analyzing the incorporation of isoprenoid precursors and intermediates into various end products (Disch et al., 1998; Hartmann and Bach, 2001; Hoeffler et al., 2002; Hemmerlin et al., 2003). The latter is due to the extremely high productivity of BY-2 cell suspensions, which have a cell division cycle of only 14 h (Nagata et al., 1992). This short cell division cycle guarantees high metabolic flux rates through the MVA and MEP pathways to end products (i.e., sterols, isoprenylated proteins, etc.). To further these studies, we created plasmids expressing GFP fused to the C-terminal domain of the rice calmodulin CaM61 (accession number U37936). In contrast with soluble calmodulins, which are highly conserved proteins in eukaryotes, including humans, *Drosophila*, and *Arabidopsis*, CaM61 from rice, like its homolog from petunia (CaM53) (Rodríguez-Concepción et al., 1999), contains a

C-terminal domain with a series of basic amino acid residues (BD) followed by a CaaX isoprenylation motif (CVIL). This tetrapeptide sequence is predicted to be a substrate for PGGT 1. Using mRNA from 4-d-old rice seedlings, we amplified a cDNA by RT-PCR encoding this CaM61 C-terminal domain (comprising 45 amino acid residues). The GFP coding sequence was then fused in frame to the 5′ end of the CaM61 C-terminal domain, and the resulting GFP fusion construct was integrated into the vector pTA7001 (Aoyama and Chua, 1997), where it was placed under the control of a promoter that is gradually inducible by dexamethasone. The corresponding plasmid, pTA-GFP-BD-CVIL, was used for stable transformation of BY-2 cells by *Agrobacterium tumefaciens*–mediated T-DNA transfer according to standard protocols. An additional GFP fusion protein was generated by site-directed mutagenesis in which the Cys of the CVIL motif was replaced by Ser (GFP-BD-SVIL). In addition to a construct
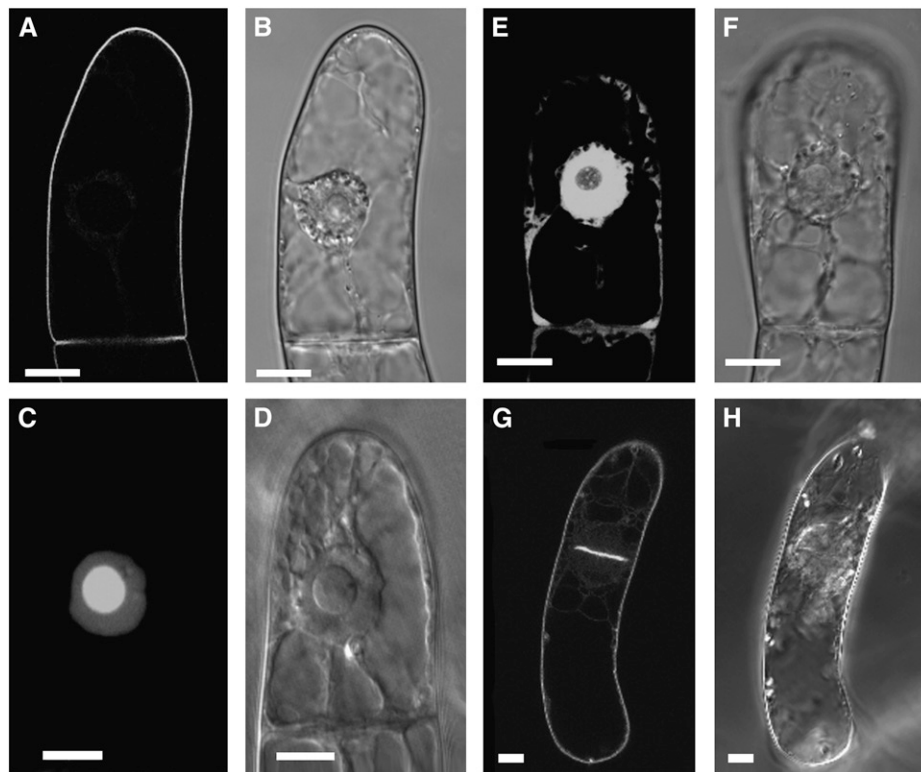
Figure 1. Localization of GFP Fusion Proteins to Subcellular Structures in Transformed BY-2 Cells.

Stably transformed BY-2 cells in the stationary phase were diluted into fresh medium and treated under standard conditions, which are described in Results. Bars = 10 μm.
(A) GFP, fused at its C terminus to the C terminus of rice calmodulin CaM61, which bears a basic domain (BD) and a CVIL geranylgeranylation motif (GFP-BD-CVIL). The resulting fluorescence is exclusively localized to the periphery of the cell.
(B) The same cell as in **(A)** in white light mode, indicating structural details, especially the position of the nucleus.
(C) Expression of a fusion protein that cannot be geranylgeranylated due to the replacement of the Cys residue in the isoprenyltransferase recognition motif by Ser (GFP-BD-SVIL). This substitution causes mislocalization of GFP-BD-CVIL to the nucleoplasm and nucleolus.
(D) The same cell as in **(C)** in white light phase contrast mode, indicating the localization of the nucleus and the nucleolus.
(E) Expression of GFP alone, with GFP fluorescence in cytoplasmic strands and nucleoplasm, but not the nucleolus.
(F) The same cell as in **(E)** in white light mode.
(G) A cell in the process of division, with accumulation of GFP-BD-CVIL in the newly forming cell plate.
(H) The same cell as in **(G)** in white light mode.
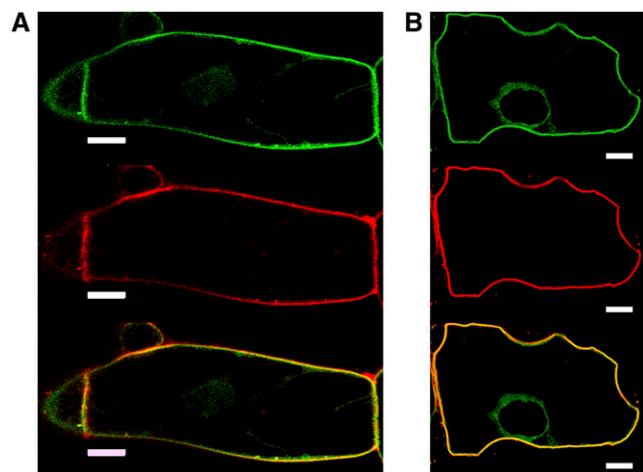
Figure 2. Localization of GFP-BD-CVIL to the Plasma Membrane in BY-2 Cells.

GFP-BD-CVIL expression was induced for 15 h with 10 μM dexamethasone before treatment with the fluorescent marker FM4-64 (6.7 μg/mL). The green channel was set for detection of GFP (top panel) and the red channel for detection of the PM marker FM4-64 (middle panel). Merged images are shown in yellow and indicate colocalization of GFP-BD-CVIL and FM4-64 (bottom panel). Bars = 10 μm.

(A) In the absence of 0.23 M D-mannitol.

(B) In the presence of 0.23 M D-mannitol, which induces plasmolysis. The images show single optical sections through the center of the cell, including the nucleus.

expressing GFP alone, this GFP construct served as a non-geranylgeranylated control.

Under standard conditions, expression of proteins was induced by the addition of 10 μM (final concentration) dexamethasone, and, after 15 h, the transformed BY-2 cells were subjected to microscopic analysis. These conditions were found to be optimal for the experiments described in this article. When the GFP-BD-CVIL fusion protein was expressed and isoprenylated in vivo, it was strictly localized to the periphery of BY-2 cells (Figures 1A and 1B). This was in sharp contrast with the subcellular localization of GFP-BD-SVIL, which cannot be isoprenylated in vivo and resulted in green fluorescence in the nucleoplasm and, more intensely, in the nucleolus (Figures 1C and 1D). This pattern of fluorescence was also clearly distinguishable from the localization of unmodified GFP, which predominantly accumulated in the cytosol and in the nucleoplasm, but not in the nucleolus (Figures 1E and 1F). In initial experiments, we verified that expression of GFP and GFP fusions was not toxic to BY-2 cells. Indeed, cells expressing GFP-BD-CVIL were observed in the process of mitosis, and, during cytokinesis, the newly formed cell plate appeared to be labeled by the geranylgeranylated GFP fusion protein (Figures 1G and 1H). To test the hypothesis that the peripheral localization of GFP-BD-CVIL was exclusively due to the integration of the protein into the plasma membrane, we used two approaches: first, by colocalization of GFP fluorescence with the red fluorescent dye FM4-64 (6.7 μg mL^{-1}), which has been described as a specific stain for the plasma membrane (Bolte et al., 2004); and, second, by inducing

plasmolysis with 0.23 M mannitol in the presence of FM4-64. The high osmoticum led to a detachment of the plasma membrane from the cell wall and maintained the colocalization of GFP-BD-CVIL and FM4-64 (Figure 2). These experiments confirmed the prediction that the C-terminus of rice CaM61 is sufficient, as in the case of petunia CaM53 (Rodríguez-Concepción et al., 1999), to target GFP to the plasma membrane.

In Vivo Inhibition of GFP-BD-CVIL Geranylgeranylation

The experiments described above provided a tool for visualizing in transformed BY-2 cells the impact of geranylgeranylation, or lack of geranylgeranylation, on GFP-BD-CVIL protein localization. Bearing in mind the unresolved question of the biochemical origin(s) of the GGPP used for protein geranylgeranylation, we made use of inhibitors that either block the MVA pathway (mevinolin [MV]) or the MEP pathway (fosmidomycin [Fos]) (Hemmerlin et al., 2003). Of course, it was necessary to establish the best conditions, such as time of incubation in the presence of inhibitors and time of dexamethasone induction of gene expression. The standard protocol thus established was as follows: 7-d-old cells in the stationary phase of cell culture were diluted fivefold into fresh medium, and 3 mL aliquots were incubated for 3 h in the presence of inhibitors, followed by a 15-h induction of GFP-BD-CVIL expression with 10 μM dexamethasone.
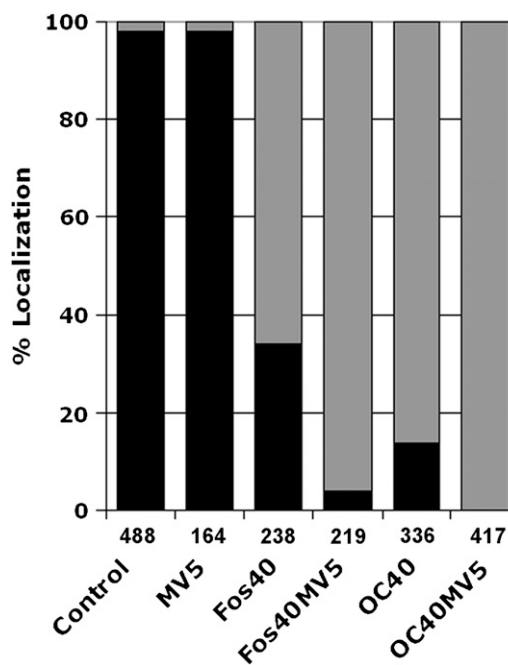
Figure 3. Quantitative Analyses of GFP-BD-CVIL Localization in BY-2 Cells Treated with MEP and MVA Pathway Inhibitors.

Percentage of GFP-BD-CVIL localized to the plasma membrane and nucleus/nucleolus in the presence of MV (5 μM), Fos (40 μM), or OC (40 μM). Black bars: percentage of cells showing plasma membrane localization. Gray bars: percentage of cells with partial or complete delocalization to the nucleus/nucleolus. The number of cells analyzed is indicated under each column.
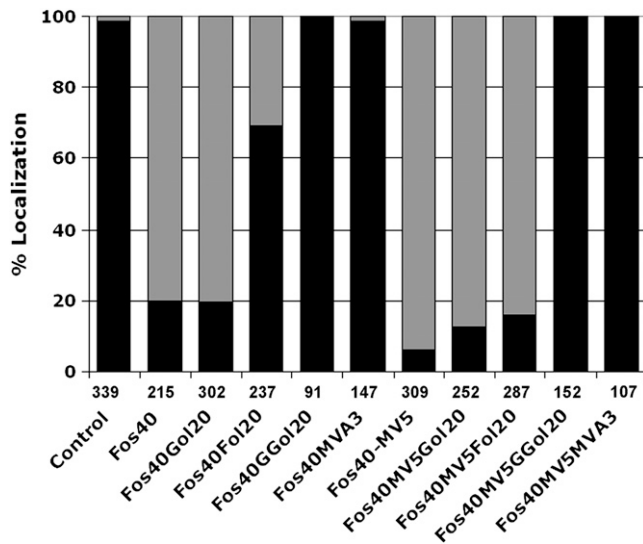
Figure 4. Chemical Complementation of Inhibitor-Induced GFP-BD-CVIL Delocalization from the Plasma Membrane to the Nucleus with MVA (3 mM) or Prenols (20 μM).

Black bars: percentage of cells showing plasma membrane localization. Gray bars: percentage of cells with partial or complete delocalization to the nucleus/nucleolus. The number of cells analyzed is indicated under each column. Fos40, Fos (40 μM); MV5, MV (5 μM); Gol20, geraniol (20 μM); Fol20, farnesol (20 μM); GGol20, geranylgeraniol (20 μM); control, transformed cells without any inhibitor treatment, displaying ~99% plasma membrane localization.

When BY-2 cells expressing GFP-BD-CVIL were treated for 3 h with 5 μM MV prior to dexamethasone induction, a concentration known to completely abolish cell division (Hemmerlin and Bach, 1998) and presumed to deplete cells of MVA and MVA-derived pathway intermediates, there was little or no effect on the predominant localization of green fluorescence at the cell periphery (Figure 3; see Supplemental Table 1 online). Previous observations (Hemmerlin et al., 2003) suggested the possibility that, within a time scale of <15 h after induction of GFP-BD-CVIL expression, export of MEP-derived compounds to the cytosol might permit geranylgeranylation of GFP-BD-CVIL. To test this hypothesis, transformed BY-2 cells were also treated with Fos at 40 μM, which resulted in a dramatic translocation of GFP-BD-CVIL to the nucleus, with traces of fluorescence localized to the plasma membrane (Figure 3; see Supplemental Table 1 online). Application of both inhibitors completely abolished integration of GFP-BD-CVIL into the plasma membrane, suggesting that some crosstalk between the pathways must exist, as demonstrated for the biosynthesis of diterpenoid ginkgolides (Schwarz and Arigoni, 1999) and, more recently, for the biosynthesis of dolichols (Skorupinska-Tudek et al., 2008). Nevertheless, the dominant contribution of the MEP pathway to the synthesis of the geranylgeranyl moiety for isoprenylation of the GFP-BD-CVIL reporter protein was clear.

To support the hypothesis that plastidial isoprenoid synthesis is required for the geranylgeranylation of GFP-BD-CVIL, cells were treated with oxoclomazone (OC; also referred to as

ketoclomazone; Zeidler et al., 2000; Sakakibara et al., 2005), a derivative of the herbicide clomazone (also referred to as FMC 57020 or dimethazone). The latter was recognized as blocking the MEP pathway at a step before the formation of phytoene (Sandmann and Böger, 1989; Lange et al., 2001). Thus, OC may inhibit an enzyme in the MEP pathway that catalyzes a reaction preceding isopentenyl diphosphate (IPP) and dimethylallyl diphosphate synthesis, such as 1-deoxy-D-xylulose 5-phosphate synthase (DXS) (Müller et al., 2000; Zeidler et al., 2000). In our system, the compound exerted an effect like, but greater than, Fos (Figure 3; see Supplemental Table 1 online), thereby validating the use of transformed BY-2 cells to visualize the impact of well-characterized, as well as uncharacterized, inhibitors that affect either the plastidial (and/or cytosolic) synthesis of isoprenyl diphosphates necessary for isoprenylation of CaaX proteins or act directly on the process of protein isoprenylation.

Chemical Complementation

To confirm the significance of the observations described above, we chemically complemented the Fos inhibition of GFP-BD-CVIL plasma membrane localization (alone and in combination with MV) with isoprenoid intermediates and end products in their dephosphorylated forms (i.e., to facilitate uptake into cells). Accordingly, geraniol (Gol), farnesol (Fol), and geranylgeraniol (GGol), each at 20 μM, and MVA, at 3 mM, were added at the time
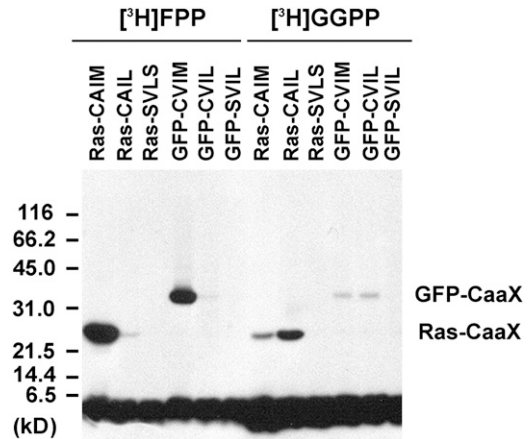
Figure 5. In Vitro Isoprenylation of Modified GFP Fusion Proteins by BY-2 Cell-Free Extracts.

GFP fusion proteins were expressed in *E. coli* and tested for in vitro isoprenylation using cell-free extracts from 3-d-old BY-2 cells as a source of protein isoprenyltransferases and [³H]-FPP or [³H]-GGPP as isoprenyl diphosphate substrates. For comparison, Ras fusion proteins were also isoprenylated in vitro. Ras-CAIM is recognized by PFT, whereas Ras-CAIL is recognized by PGGT 1. By contrast, Ras-SVLS is not recognized by any known protein isoprenyltransferase. GFP-BD-CVIL was predicted to be a substrate of PGGT 1, whereas GFP-CVIM was predicted to be a substrate of PFT. GFP-SVIL served as a control protein that cannot be isoprenylated. The positions of GFP-CaaX and Ras-CaaX, which agree with the predicted molecular masses, are indicated. The broad band on the bottom of the gel corresponds to free radiolabeled substrate.

of dexamethasone induction (Figure 4; see Supplemental Table 2 online). While GoI did not significantly overcome inhibition of GFP-BD-CVIL plasma membrane localization by Fos, FoI exhibited a 62% capacity to counteract the effect of Fos [(69 − 20)/(99 − 20) × 100], and an 11% capacity to block the effect of both inhibitors [(16 − 6)/(99 − 6) × 100]. By contrast, 20 μM GGoI fully complemented the inhibitory effect of Fos under all conditions (Figure 4; see Supplemental Table 2 online), and 100% recovery of GFP fluorescence to the cell periphery was achieved at concentrations of GGoI as low as 5 μM. The concentration of MVA required to achieve a similar degree of complementation was 3 mM. The specificity of the GGoI effect is remarkable, suggesting efficient conversion to the corresponding diphosphate in tobacco BY-2 cells.

In Vitro Isoprenylation of GFP Fusion Proteins by BY-2 Cell-Free Extracts

Protein isoprenyltransferase substrate specificities are high, but not absolute (Trueblood et al., 1993), and a strongly active farnesyltransferase might weakly accept a protein substrate with a C-terminal CVIL motif for attachment of a farnesyl residue, which might be sufficient for anchoring the protein into the plasma membrane. To rule out this possibility, modified His$_6$-GFP-BD-CVIL proteins were expressed in *Escherichia coli* and isoprenylated in vitro using BY-2 cell extracts as a source of protein isoprenyltransferases (Figure 5). As controls, rat sarcoma (RAS) proteins with known CaaX sequences were used (Randall et al., 1993). As shown in Figure 5, RAS-CAIM and GFP-BD-CVIM were strongly farnesylated in the presence of BY-2 extracts, whereas RAS-CAIL and GFP-BD-CVIL were predominantly geranylgeranylated. As expected, RAS-SVLS and GFP-

BD-SVIL controls were not detectably isoprenylated in the presence of BY-2 extracts. The positions of isoprenylated GFP-CaaX and Ras-CaaX agree with the predicted molecular masses of 31.7 and 26.0 kD, respectively. These results demonstrate that, as in other systems, protein isoprenyltransferases from BY-2 cells exhibit high selectivity for CaaX protein substrates.

In Vivo Isoprenylation of GFP Fusion Proteins in BY-2 Cells

To definitively establish in vivo geranylgeranylation, or loss of geranylgeranylation, of His$_6$-GFP-BD-CVIL in the absence or presence of MEP pathway inhibitors, respectively, His$_6$-GFP-BD-CVIL expressed in *E. coli* was compared with His$_6$-GFP-BD-CVIL from extracts of BY-2 cells treated with or without inhibitors. These proteins were resolved by SDS-PAGE, and the region of the gel containing GFP was identified by immunoblot analysis, cut and digested with the endoprotease Asp-N. Peptides were then extracted, fractionated, and submitted for matrix-assisted laser-desorption ionization time of flight (MALDI-TOF) peptide mass fingerprinting and MALDI-TOF tandem mass spectrometry (MS/MS) peptide mass sequencing. Unprenylated, farnesylated, and geranylgeranylated His$_6$-GFP-BD-CVIL proteins were predicted to produce monoisotopic C-terminal peptide fragments of 2756.4800, 2784.5620, and 2852.4431 D, respectively. As shown in Figure 6, a peptide with a parent ion of 2852.680 mass-to-charge ratio (m/z) was detected from control BY-2 cells, supporting the conclusion that His$_6$-GFP-BD-CVIL is geranylgeranylated in vivo. By contrast, a peptide with a parent ion of 2756.6200 m/z was detected from BY-2 cells treated with Fos; Figure 6), confirming the essential role of the MEP pathway in GFP-BD-CVIL geranylgeranylation. The peptide sequences of the parent ions ([M+H]$^+$ = 2852.6800 and [M+H]$^+$ = 2756.6200)
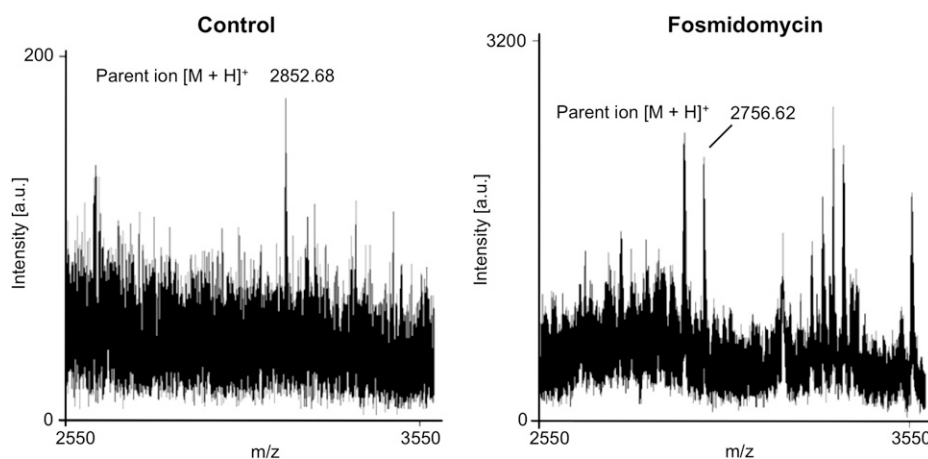
Figure 6. In Vivo Characterization of His$_6$-GFP-BD-CVIL Isoprenylation by MS Analysis of His$_6$-GFP-BD-CVIL–Derived Peptides.

Solubilized total membrane and supernatant fractions from tobacco BY-2 cells induced to express His$_6$-GFP-BD-CVIL were resolved by SDS-PAGE, and recombinant His$_6$-GFP-BD-CVIL was cut from the gel, digested with Asp-N, and extracted and fractionated by solid-phase extraction for MALDI-TOF MS peptide mass fingerprinting and MALDI-TOF MS/MS peptide mass sequencing (detailed in Supplemental Figure 1 online). A significant peak was detected at an m/z of 2852.68, which corresponded to the predicted mass of a geranylgeranylated, methylated C-terminal His$_6$-GFP-BD-CVIL peptide. Peaks at an m/z of 2756.62 or an m/z of 2784.56, which correspond to unprenylated and farnesylated peptides, respectively, were not detected in the absence of inhibitors (Control). However, a significant peak was detected at an m/z of 2756.62 from tobacco BY-2 cells treated with Fos.

were confirmed by MALDI-TOF MS/MS (see Supplemental Figure 1 online).

Isoprenylation and Localization of GFP-CaM61 and GFP-BD-CVIL Fusion Proteins

We were surprised by the discrepancy between our observations using GFP fused to the basic domain and CVIL motif of CaM61 and those of Dong et al. (2002) using GFP fused to the full-length CaM61. To investigate this discrepancy further, we obtained the *Agrobacterium* strain harboring the GFP-CaM61 fusion plasmid used by Dong et al. (2002) for agroinfiltration of tobacco (*Nicotiana benthamiana*) leaves and stable transformation of BY-2 cells. When transiently transformed epidermal cells of *N. benthamiana* were examined by confocal microscopy, GFP fluorescence was associated with the cell periphery, but also with cytoplasmic strands and the nucleus (Figure 7A). At higher magnifications, it was evident that fluorescence was associated with the nucleus, but not with the nucleolus (Figure 7B). By contrast, when the same experiment was performed with the truncated GFP-BD-CVIL construct developed in this study as a reporter for protein geranylgeranylation in BY-2 cells, plasma membrane association was much more clear (Figure 7C), and labeling was more pronounced in the nucleolus (Figure 7D). Essentially the same observations were made with newly trans-

formed BY-2 cells (Figure 8). Expression of the full-length GFP-CaM61 protein resulted in association of GFP fluorescence with intracellular membranes (i.e., endoplasmic reticulum [ER] and perinuclear membranes), plasma membrane, and cytoplasmic strands (Figure 8A), whereas expression of GFP-BD-CVIL resulted in nearly exclusive association of GFP fluorescence with the plasma membrane (Figure 8B). MV treatment, using conditions described by Dong et al. (2002), had little or no effect on the localization of GFP-CaM61 (Figure 8C) and GFP-BD-CVIL (Figure 8D). Fos treatment, on the other hand, caused partial translocation of GFP-CaM61 to the nucleus, but not the nucleolus (Figure 8E), and translocation of GFP-BD-CVIL to both the nucleus and the nucleolus (Figure 8F). Treatment with both MV and Fos increased the nuclear localization of GFP-CaM61 (Figure 8G) and caused almost complete translocation of GFP-BD-CVIL to the nucleus and nucleolus (Figure 8H). These results demonstrate that our reporter system is much more suitable for visualizing protein isoprenylation in vivo and show the predominant accumulation of unprenylated GFP-BD-CVIL (i.e., in the presence of Fos) and GFP-BD-SVIL in nucleoli (Figure 1). Addition of Ca^{2+} or the calmodulin inhibitor calmidazolium (cf. Merret et al., 2007) did not affect the localization of GFP-CaM61 or GFP-BD-CVIL (see Supplemental Figure 2 online). Furthermore, the MV used in these experiments, and all experiments herein reported, was biologically active, as judged by its effect on the growth of BY-2 cell cultures (see Supplemental Figure 3 online).
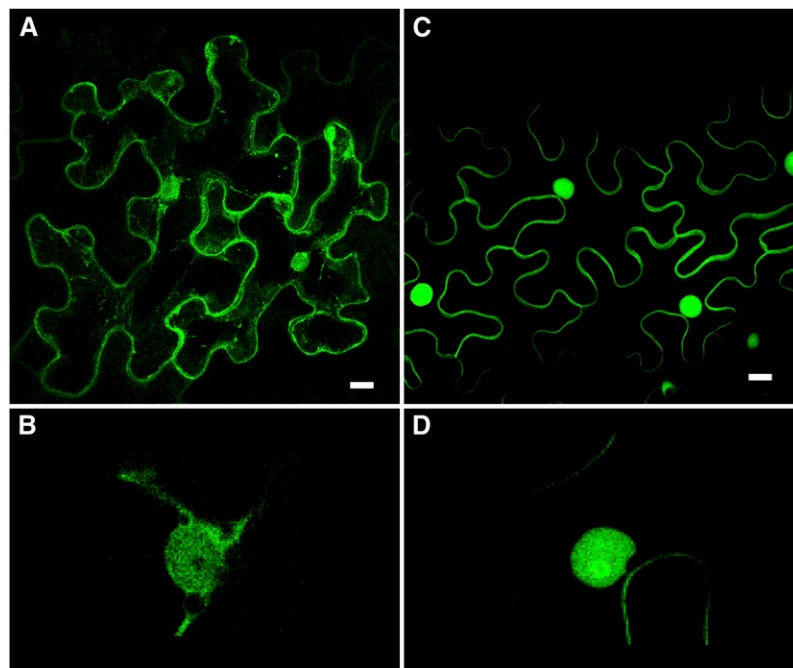
Figure 7. Localization of GFP-CaM61 and GFP-BD-CVIL in Epidermal Cells of *N. benthamiana* Leaves.

(A) Localization of GFP-CaM61, showing GFP fluorescence associated with the cell periphery, nucleus, and cytoplasmic strands.
(B) At higher magnification, GFP-CaM61 is observed in the nucleus, but not the nucleolus.
(C) Localization of GFP-BD-CVIL, showing GFP fluorescence associated with the plasma membrane and nucleus, but not cytoplasmic strands.
(D) At higher magnification (threefold electronic zoom), GFP-BD-CVIL is observed to be concentrated in the nucleolus.
Bars = 10 μm. [See online article for color version of this figure.]
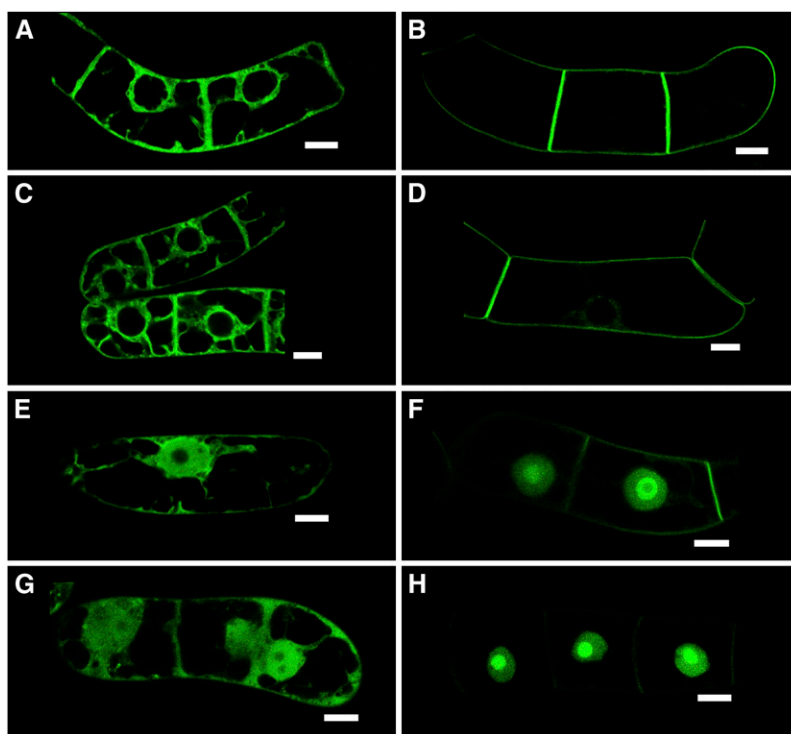
Figure 8. Localization of GFP-CaM61 and GFP-BD-CVIL in BY-2 Cells.

(A) Localization of GFP-CaM61 in BY-2 cells, showing GFP fluorescence associated with ER and perinuclear membranes, plasma membrane, and cytoplasmic strands.

(B) Localization of GFP-BD-CVIL in BY-2 cells, showing GFP fluorescence associated exclusively with the plasma membrane.

(C) Localization of GFP-CaM61 in BY-2 cells treated with MV as described by Dong et al. (2002), showing GFP fluorescence associated with ER and perinuclear membranes, plasma membrane, and cytoplasmic strands.

(D) Localization of GFP-BD-CVIL in BY-2 cells treated with MV as described by Dong et al. (2002), showing GFP fluorescence associated with the plasma membrane (faint fluorescence is also seen in the nucleus).

(E) Localization of GFP-CaM61 in BY-2 cells treated with Fos, showing partial translocation of GFP fluorescence to the nucleus, but not the nucleolus.

(F) Localization of GFP-BD-CVIL in BY-2 cells treated with Fos, showing translocation of GFP fluorescence to the nucleus and nucleolus.

(G) Localization of GFP-CaM61 in BY-2 cells treated with MV and Fos, showing increased translocation of GFP fluorescence to the nucleus.

(H) Localization of GFP-BD-CVIL in BY-2 cells treated with MV and Fos, showing almost complete translocation of GFP fluorescence to the nucleus and nucleolus.

Bars = 10 μm. [See online article for color version of this figure.]

A Bioassay for the Identification of MEP Pathway and PGGT 1 Inhibitors

As predicted (Hemmerlin et al., 2006), DX restored plasma membrane localization of His$_6$-GFP-BD-CVIL in the presence of OC (Figure 9). The ability of DX to bypass the DXS reaction in the presence of OC confirmed the prediction that OC inhibits DXS (see also Sakakibara et al., 2005). Not surprisingly, DX did not complement the inhibition of MEP synthase by Fos. The bioassay shown in Figure 9 is equally sensitive to inhibitors of PGGT 1; indeed, the PGGT 1 inhibitor GGti-2133 caused His$_6$-GFP-BD-CVIL translocation to the nucleus/nucleolus (Figure 9). However, in contrast with MEP pathway inhibitors, GGti-2133 inhibition of His$_6$-GFP-BD-CVIL plasma membrane localization was not complemented by 5 μM GGol. Thus, inhibitors of different MEP pathway enzymes, or PGGT 1, can be readily distinguished by chemical complementation.

The results shown in Figure 9 establish a convenient bioassay for the detection of novel MEP pathway inhibitors that are efficiently absorbed by BY-2 cells. This has clinical and agricultural significance, as MEP pathway inhibitors are potentially useful as novel antibiotics, antimalarial drugs, or herbicides (Lichtenthaler et al., 2000; Zeidler et al., 2000; Rodríguez-Concepción, 2004; Rohmer et al., 2004; Kuntz et al., 2005). To screen for novel MEP pathway inhibitors, transformed BY-2 cells are introduced into 96-well plates, treated with chemicals from a combinatorial chemical library, induced to express GFP-BD-CVIL with dexamethasone, and examined by confocal microscopy. Inhibition of plasma membrane localization of GFP-BD-CVIL can then be used as a means of identifying compounds that either inhibit the MEP pathway or PGGT 1, and restoration of plasma membrane localization by GGol can be used to confirm those that inhibit the MEP pathway. The utility of
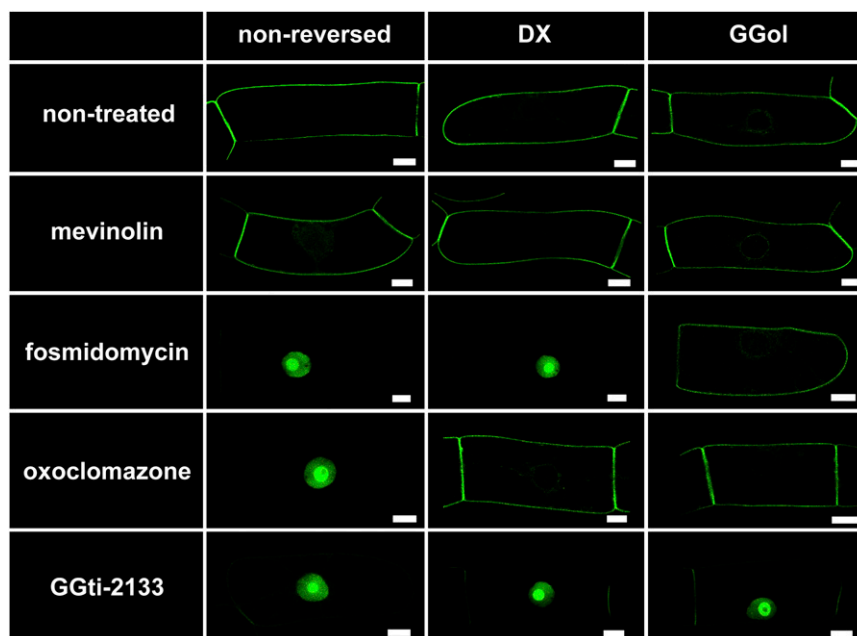
Figure 9. A Bioassay for the Identification of MEP Pathway and PGGT 1 Inhibitors.

His$_6$-tagged GFP-BD-CVIL localization in transformed BY-2 cells. His$_6$-GFP-BD-CVIL was localized to the periphery of transformed BY-2 cells in the absence of inhibitors. MV (5 μM) exerted no detectable effect on His$_6$-GFP-BD-CVIL localization. By contrast, Fos (40 μM) caused a dramatic translocation of His$_6$-GFP-BD-CVIL to the nucleus/nucleolus. GGol (5 μM), but not DX (0.5 mM), reversed this effect (Fos inhibits MEP synthase). OC (10 μM) also caused a dramatic translocation of His$_6$-GFP-BD-CVIL to the nucleus/nucleolus, but GGol and DX reversed this effect (OC inhibits DXS). In addition, GGti-2133 (30 μM) caused His$_6$-GFP-BD-CVIL to accumulate in the nucleus/nucleolus, but was not reversed by GGol or DX (GGti-2133 inhibits PGGT 1). Bars = 10 μm. [See online article for color version of this figure.]

this high-throughput screening procedure is shown in Figure 10. BY-2 cells expressing His$_6$-tagged GFP-BD-CVIL were treated with or without OC (30 μM), MV (5 μM), or a combination of both inhibitors, followed by fluorescence microscopy at low resolution. Control and MV-treated cells were apparently identical (Figure 10), with GFP fluorescence at the periphery of the cells, especially the boundary between neighboring cells, and to some extent the perinuclear membrane, whereas the GFP fluorescence in OC-treated cells was almost exclusively nuclear. The combination of MV and OC did not visibly affect GFP fluorescence compared with OC alone.

DISCUSSION

For years, it was assumed that the FPP and GGPP used in plant cells for protein isoprenylation was derived from the MVA pathway (Crowell, 2000). This assumption was based on early observations that incubation of tobacco BY-2 cells or spinach seedlings with radiolabeled MVA resulted in the incorporation of radioactivity into proteins (Randall et al., 1993; Shipton et al., 1995). Even after the discovery and elucidation of the plastidial MEP pathway (cf. Rohmer, 1999; Rodríguez-Concepción and Boronat, 2002), the apparently cytosolic location of protein isoprenyltransferases suggested that the isoprenyl diphosphates used for protein isoprenylation were also synthesized in

the cytosol. However, this assumption was challenged by the observation that low molecular weight proteins could be radiolabeled with [^{14}C]DX (Hemmerlin et al., 2003). This labeling supports the hypothesis that IPP, GPP, or GGPP can be exported from plastids to the cytosol, which would then efficiently be used for isoprenylation of proteins. Here, it is definitively shown that the GGPP used for geranylgeranylation of a GFP-BD-CVIL protein is predominantly derived from the plastidial MEP pathway in tobacco BY-2 cells (Figures 3, 4, 9, and 10).

It is not clear whether plastidial or cytosolic GGPP synthases (GGDS) are necessary for protein isoprenylation in BY-2 cells. If IPP or GPP are exported, then a cytosolic GGDS is required for protein geranylgeranylation, but if GGPP is exported, a plastidial GGDS is required (Figure 11). The fact that *Arabidopsis* possesses several GGDS enzymes (Okada et al., 2000), two of which were reported to be localized to the ER, two to plastids, and one to mitochondria, does not conflict with the results shown here because GGDS genes are differentially expressed in a tissue- and development-specific manner, and it is possible that plastidial forms of GGDS are predominant in BY-2 cells. Plastids in BY-2 cells are generally considered to be proplastids, although cytokinin treatment can stimulate their development into amyloplasts (Miyazawa et al., 2002), where significant amounts of starch are produced. Consequently, the metabolic flux through the MEP pathway is not directed toward producing chlorophylls, carotenoids, plastoquinones, and other isoprenoids
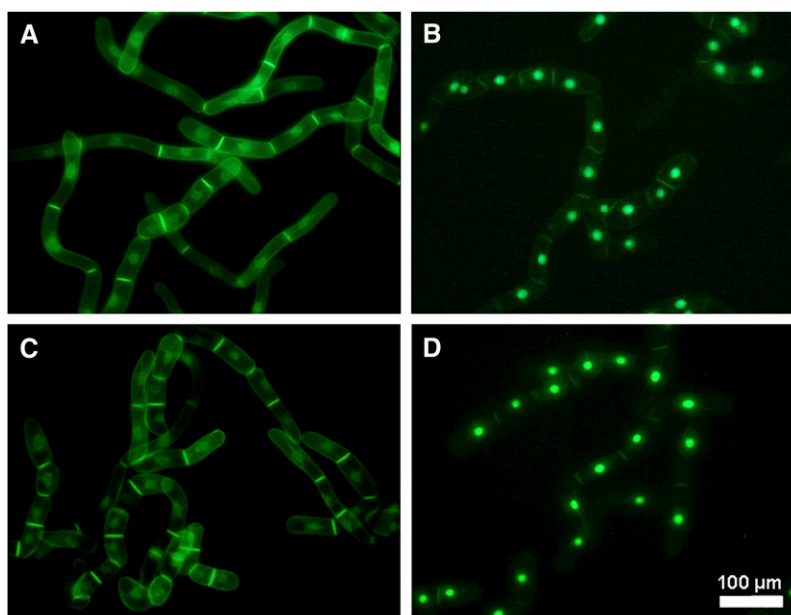
Figure 10. Reproducibility of Effects on a Random Collection of BY-2 Cells.

Fluorescence images at low resolution of large numbers of cloned BY-2 cells expressing His$_6$-GFP-BD-CVIL (Nikon DXM11200 CCD color camera, 20 × 0.45 objective; filters: EX460-500, DM505, EM510-560). [See online article for color version of this figure.]
**(A)** Untreated cells.
(B) to **(D)** Cells treated with 30 μM OC **(B)**, 5 μM MV **(C)**, and 30 μM OC plus 5 μM MV **(D)**.

characteristic of differentiated plastids. This allows for carbon flux through the MEP pathway to be directed toward processes such as protein isoprenylation. The situation in green leaves may be entirely different because carbon flux through the MEP pathway is directed toward producing photosynthetic pigments and electron carriers. Thus, the question arises: Is the GGPP necessary for protein geranylgeranylation derived from the MEP pathway in green leaves, roots, or tomato fruits? Perhaps the existence of both plastidial and cytosolic forms of GGDS (Okada et al., 2000) suggests that the GGPP used for protein geranylgeranylation has different biosynthetic origins in different tissues. Analysis of GGDS mutants of *Arabidopsis* may help to answer this question.

The MEP pathway origin of the GGPP used for protein isoprenylation in our test system is an intriguing result in view of the fact that, in a recent study using vesicles prepared from envelope membrane fractions of spinach, kale, and Indian mustard (*Brassica juncea*) plastids, it was shown that unidirectional transport of IPP and GPP occurred from the plastid to the cytosol, while transport of intermediates like FPP and GGPP was less efficient (Bick and Lange, 2003). Several published studies support the hypothesis that IPP, GPP, and GGPP are transported between the cytosolic and plastidial compartments, with a preference for transport from the plastid to the cytosol (Hemmerlin et al., 2003; Skorupinska-Tudek et al., 2008). This observation corroborates in vivo observations (Kasahara et al., 2002, 2004; Laule et al., 2003; Sakakibara et al., 2005) with inhibitor-treated *Arabidopsis* seedlings, cell cultures of Madagascar periwinkle (*Catharanthus roseus*) (Schuhr et al., 2003), and BY-2 cells (Hemmerlin et al.,

2003). However, in the two latter studies, exogenous MVA was, to some extent, incorporated into plastids and used to produce plastidial isoprenoids. Under stress conditions, the export of MEP-derived intermediates might be required to satisfy the need for the production of defense-related sesquiterpenoids in the cytosolic compartment (Piel et al., 1998; Adam et al., 1999). Dudareva et al. (2005) showed that, in the epidermis of snapdragon petals, only the plastid-localized MEP pathway is active in the formation of volatile terpenes and provides IPP precursors for both plastidial monoterpene and cytosolic sesquiterpene biosynthesis. If such an exported intermediate were to be allylic GPP, a cytosolic farnesyl diphosphate synthase (FDS) would be expected to catalyze its conversion to FPP. Alternatively, in BY-2 cells, a cytosolic FDS might catalyze GGPP synthesis, and, if present, GGDS might catalyze the conversion of exported GPP to GGPP. Under some conditions, FDS enzymes are capable of synthesizing GGPP in vitro (Eberhardt and Rilling, 1975). Furthermore, it was recently shown that maize (*Zea mays*) endosperm cDNAs coding for FDS, when expressed in an engineered *E. coli* strain, provided the GGPP needed for carotenoid formation (Cervantes-Cervantes et al., 2006).

A system for phosphorylation of Fol and GGol in plant cells has been described (Thai et al., 1999), and incorporation of radiolabeled Fol into ubiquinone in BY-2 cells (Hartmann and Bach, 2001) is indicative of double phosphorylation preceding transport into mitochondria. Our observations are consistent with the prediction that this CTP/GTP-dependent phosphorylation system will not accept Gol as a substrate, but will accept GGol and Fol (Thai et al., 1999), thus preventing the conversion of Gol to
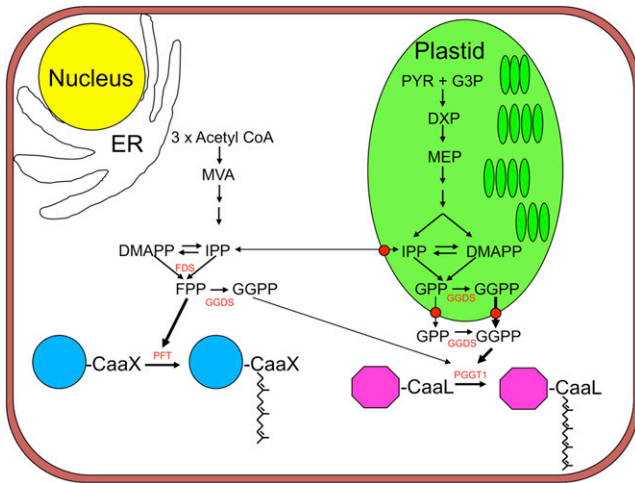
Figure 11. Biosynthetic Origins of Farnesyl Diphosphate and Geranyl-geranyl Diphosphate in BY-2 Cells for Protein Farnesylation and Geranylgeranylation, Respectively.

CaaX, isoprenylation motif; DMAPP, dimethyl allyl diphosphate; DXP, 1-deoxy-D-xylulose 5-phosphate; FDS, farnesyl diphosphate synthase; GGDS, geranylgeranyl diphosphate synthase; G3P, D-glyceraldehyde 3-phosphate; GPP, geranyl diphosphate; IPP, isopentenyl diphosphate; PYR, pyruvate.

GGPP for use in protein geranylgeranylation. As chemical complementation by GGol occurred at much lower concentrations than any other compound tested, its effect is very specific in view of the possibility that the cellular concentration could be even lower (i.e., due to limited uptake). The ability of 20 μM Fol to partially complement Fos inhibition of GFP-BD-CVIL plasma membrane localization was reduced by parallel inhibition of the MVA pathway in the presence of MV. There are two possible interpretations of this result: (1) conversion of exogenous FPP to GGPP requires MVA-derived IPP, or (2) Fol induction of the MVA pathway via increased 3-hydroxy-3-methylglutaryl CoA reductase activity (Hemmerlin and Bach, 2000), import of excess cytosolic IPP into plastids, conversion of IPP to GPP or GGPP, and reexport of GPP or GGPP to the cytosol rescues the plasma membrane localization of GFP-BD-CVIL. The ability of high concentrations of MVA (3 mM; 600 times higher than that of GGol) to restore plasma membrane localization of GFP-BD-CVIL in the presence of Fos (alone or in combination with MV) is also presumably due to import of excess cytosolic IPP into plastids (high concentrations of MVA bypass the rate-limiting step of the MVA pathway [Bach, 1995]), conversion to GPP or GGPP, and reexport.

The in vitro protein isoprenylation assays shown in Figure 5 suggest that PFT and PGGT 1 from BY-2 cells exhibit substrate preferences that are not absolute. However, the in vivo isoprenylation results shown in Figure 6 indicate that GFP-BD-CVIL is specifically geranylgeranylated in BY-2 cells, with no detectable farnesylation. These results suggest that the specificity of protein isoprenylation is higher in vivo than in vitro. A likely explanation for this is that in vitro isoprenylation reactions are performed with an excess of protein and isoprenyl diphosphate substrates,

whereas in vivo concentrations of these substrates are likely to be much lower. Thus, substrates with weak affinities for PFT or PGGT 1 are more likely to be aberrantly isoprenylated in vitro.

Rodríguez-Concepción et al. (1999) showed that, in epidermal cells of *Arabidopsis* plants expressing GFP fused to the C-terminus of petunia CaM53 (GFP-CaM53), some GFP fluorescence was always present in the nucleus, with or without MV treatment. In this study, a potato virus X (PVX) vector was used for ectopic expression of GFP-CaM53. Thus, GFP-CaM53 expression was driven by a strong promoter and the epidermal cells might not have been capable of providing sufficient amounts of isoprenyl diphosphates for complete isoprenylation of GFP-CaM53. This alone could account for the partial nuclear localization of GFP-CaM53 observed in epidermal cells of *Arabidopsis* as well as the partial nuclear localization of GFP-CaM61 and GFP-BD-CVIL observed in epidermal cells of *N. benthamiana* (Figure 7). Moreover, the translocation of GFP-CaM53 from the plasma membrane to the nucleus in the presence of high concentrations of MV (25 and 50 μM), albeit incomplete, might have been caused by the inhibitor's cytotoxicity, as previously reported (Bach and Lichtenthaler, 1983). Interestingly, when leaves were kept in the dark, GFP-CaM53 localization shifted from the plasma membrane to the nucleus, and this effect was reversed by the addition of 2% sucrose. In the dark, photosynthesis is shut down in the chloroplasts of parenchymal cells, which normally provide carbohydrates (i.e., sucrose) to neighboring epidermal cells. In epidermal cells, sucrose is metabolized to triose phosphate and pyruvate, and, because epidermal cells are nonphotosynthetic, both products are transported into plastids and supply the MEP pathway with precursor compounds. In the dark, the decreased supply of sucrose to the epidermal cells presumably results in a decreased metabolic flux rate through the MEP pathway, decreased GGPP synthesis, and decreased geranylgeranylation of GFP-CaM53. However, exogenous sucrose reverses this effect and restores the MEP pathway, GGPP synthesis, and GFP-CaM53 geranylgeranylation. Indeed, evidence abounds for transport of MEP pathway intermediates between cells and tissues (Burlat et al., 2004; Gutiérrez-Nava et al., 2004; Oudin et al., 2007).

Our results are in contrast with those of Dong et al. (2002), who expressed GFP fused to the full-length rice CaM61 and reported that MV shifted the GFP-CaM61 fusion protein from membranes to the nucleus. However, this MV-induced shift was marginal, and we were not able to reproduce the result, even when we used the same GFP-CaM61 construct (Figure 8) and the same experimental conditions (we also confirmed the biological activity of the MV we used; see Supplemental Figure 3 online). Moreover, neither calcium nor the calmodulin inhibitor calmidazolium affected the localization of GFP-CaM61 or GFP-BD-CVIL. However, our data demonstrate a minor role for the MVA pathway in GFP-BD-CVIL plasma membrane localization. Indeed, the GFP-BD-CVIL reporter system for detection of MEP pathway inhibitors is most effective in the presence of a low concentration of MV, which abolishes all traces of plasma membrane localization that potentially depend on MVA-derived GGPP.

The data shown in Figures 9 and 10 establish a rapid, visual assay for inhibitors that either inhibit the MEP pathway or PGGT 1. This assay can be adapted to high-throughput screening of

combinatorial chemical libraries for novel inhibitors of the MEP pathway. Thus, the data in Figure 9 have pharmaceutical and agricultural significance, as MEP pathway inhibitors may be useful as antibiotics, antimalarial drugs, or herbicides. Because resistance to existing antibiotics and herbicides progressively limits their usefulness, screening methods such as this will be essential for future drug development and sustainable agriculture. While this manuscript was in preparation, Simonen et al. (2008) reported a visual system similar to that described here that was used for the optical high-throughput screening of protein isoprenyltransferase inhibitors based on GFP, which was tagged with the isoprenylation motif of human H-Ras and transformed into human osteosarcoma (U-2 OS) cells.

METHODS

Plant Materials

The tobacco (*Nicotiana tabacum* cv BY-2) suspension cell culture was made available by Toshiyuki Nagata (Tokyo University, Japan) (Nagata et al., 1992). Cultivation was done as described (Hemmerlin and Bach, 1998, 2000). Rice seeds (*Oryza sativa* ssp. japonica 'Rubribarbis') were provided by the Botanical Garden of the Université Louis Pasteur and germinated for 4 d at 22°C on moistened Whatman 3MM filter paper in plastic boxes with constant light. The *Agrobacterium tumefaciens* strain LB4404 harboring the plasmid coding for GFP-CaM61 (Dong et al., 2002) was kindly provided by Wen-Hui Shen (Institut de Biologie Moléculaire des Plantes, Strasbourg, France).

Chemicals

MVA lactone, Gol, Fol, and GGol were purchased from Sigma-Aldrich. MV (Alberts et al., 1980) was a kind gift from Alfred Alberts (Merck, Rahway, NJ). Before use, the lactones of MV and MVA were converted to their open acid forms. Fos (Okuhara et al., 1980) was made available by Robert J. Eilers (Monsanto, St. Louis, MO). The peptidomimetic protein geranyl-geranylation inhibitor GGti-2133 (Vasudevan et al., 1999) was purchased from Calbiochem (Merck). OC was provided by Klaus Grossmann (BASF, Limburgerhof, Germany). The fluorochrome probe FM4-64 was provided by Molecular Probes. All other chemicals were from usual commercial sources and were of highest available purity.

Cloning of the C-Terminal End of Rice CaM61

According to standard protocols, total RNA was produced from rice seedlings (50 mg). Four micrograms were used as template for RT-PCR amplification of the coding sequence for the C-terminal basic domain/CaaX motif of rice CaM61 using CaM61F (5′-TACGAG<u>GAGCTC</u>GT-CAAGTG-3′) as a forward primer and CaM61R (5′-GCTG<u>TCTAGA</u>TTA-CAGGATCACGCACTTC-3′) as a reverse primer. These primers introduced a *Sac*I restriction site (underlined) at the 5′ end and a *Xba*I restriction site (underlined) at the 3′ end of the PCR fragment. For site-directed mutagenesis, the reverse CaM61R primer was replaced by BDSVILR (5′-GCTG<u>TCTAGA</u>TTATTACAGGATCAC**CGA**CTTC-3′) to mutate the Cys (TGC) to Ser (TCG, in bold). The PCR fragments were cloned in frame into the *Sac*I and *Xba*I sites of pGFP-MRC (Rodríguez-Concepción et al., 1999) at the C-terminal end of a synthetic GFP.

Vector Constructions and Inducible Expression of GFP Fusion Proteins

The sequence encoding the GFP-BD-CVIL fusion protein was subcloned into the *Xho*I and *Spe*I sites of the pTA7001 vector (Aoyama and Chua,

1997). To generate a *Xho*I restriction site (underlined) at the 5′ and a *Spe*I restriction site (underlined) at the 3′ end, we used the forward primer pGFPXHF (5′-AATTTT<u>CTCGAG</u>TTACGAACGATAGCCATGGTG-3′) and the reverse primer pGFPL1R (5′-CTCAGT<u>ACTAGT</u>TCAATTATTACAG-GATCACGC-3′). The reverse primer SLSp (5′-GG<u>ACTAGT</u>TTATTACAG-GATCACCGACTTCTGGCC-3′) was used to amplify the sequence corresponding to GFP-BD-SVIL, and the reverse primer pGFPSPR (5′-CCAGATCTG<u>ACTAGT</u>GAGCTAGTCCATGCC-3′) was used to amplify GFP. *Agrobacterium tumefaciens* strain LBA 4404 was used for *Agrobacterium*-mediated transformation of BY-2 cells. The transformation protocol followed that of Criqui et al. (2000), with the exception that transformed cells were clonally selected by callus induction. Stably transformed BY-2 cells were subcultured into Murashige and Skoog medium and supplemented with 113 μg mL^{-1} hygromycin B. To induce protein expression, 7-d-old BY-2 cells were diluted fivefold into fresh medium (3 mL total volume per sample) in 6-well culture cluster plates (Corning) and treated with 10 μM dexamethasone (Sigma-Aldrich), which was dissolved in 100% DMSO at a stock concentration of 30 mM. The solvent alone did not exert any measurable effect on protein expression or localization of GFP fluorescence. BY-2 cells treated with dexamethasone were placed on a rotary shaker at 140 rpm and kept in darkness at 26°C for 15 h (standard condition empirically determined). For inhibition studies, cells were treated for 3 h with inhibitors, alone or in combination, followed by induction of GFP or GFP fusion protein expression by dexamethasone for 15 h. For chemical complementation experiments, isoprenols (Gol, Fol, and GGol) or MVA were added together with dexamethasone, but otherwise the same time schedule as described above was followed.

Agroinfiltration of *Nicotiana benthamiana* Leaves

Overnight cultures of *Agrobacterium* were washed with water and suspended at an OD$_{600}$ ~1 in water containing 30 μM dexamethasone. The suspension was then infiltrated into 1-month-old *N. benthamiana* leaves, and fluorescence microscopy was performed after 30 h.

Confocal Microscopy

Fluorescent cells were counted at low magnification using a LSM510 confocal laser scanning microscope equipped with an inverted Zeiss Axiovert 100M. At confocal resolution, individual cells representative of the various populations were analyzed, and images were acquired and analyzed as described (Hemmerlin et al., 2006). At high resolution, pictures were taken such that the focal plane included the nucleus and nucleolus. Transmission images were recorded in Nomarski phase contrast mode. The fluorescence intensity of different subcellular structures and compartments (vacuole, plasma membrane, nucleus, and cytoplasm) was measured pixel-by-pixel using Image J software version 1.31 (Wayne Rasband, NIH; http://rsb.info.nih.gov/ij).

In Vitro Isoprenylation of GFP-BD-CaaX Proteins

The 843-bp DNA fragments coding for the GFP-BD-CVIL, GFP-BD-CVIM, and GFP-BD-SVIL fusion proteins were cloned into the *Nde*I and *Hind*III restriction sites of the pBAD vector (accession number U62637 from ClonTech). Restriction sites were introduced by PCR using the forward primer NdeH6CAAX-F (5′-GGAATTC<u>CCATATG</u>CATCACCATCACCAT-CACGTGAGCAAGGGCGAGGA-3′) and the reverse primer HindCVIL-R (5′-CCC<u>AAGCTT</u>GGTTACAGGATCACGCACTTCTG-3′) or HindCVIMR (5′-CCC<u>AAGCTT</u>GGTTACATGATCACGCACTTCTG-3′) or HindSVIL-R (5′-CCC<u>AAGCTT</u>GGTTACAGGATCACGGACTTCTG-3′), respectively. GFP-BD-CaaX proteins were expressed in liquid cultures of *Escherichia coli* Rosetta cells (EMD Biosciences/Novagen) containing pBAD-GFP-BD-CVIM, pBAD-GFP-BD-CVIL, or pBAD-GFP-BD-SVIL constructs. Protein inductions were performed at 22°C with 0.1% L-arabinose for

16 h. Induced cells were sedimented and resuspended in 1 mL STE buffer (150 mM NaCl, 10 mM Tris-HCl, pH 7.5, and 1 mM EDTA) containing Complete Protease Inhibitors (Roche Diagnostics). Cell disruption was accomplished by three 15-s pulses at 4°C using a Branson Sonifier 450 and a microprobe at 80% maximum power. Cell debris was removed by centrifugation at 5000g for 10 min at 4°C. In vitro protein isoprenylation was performed essentially as described (Randall et al., 1993). Ras proteins with CAIM, CAIL, or SVLS motifs at the C terminus were used as control protein substrates. Reactions were incubated for 60 min at 30°C and analyzed by SDS-PAGE and fluorography using Amplify fluorographic reagent (Amersham Biosciences) and Kodak XAR-5 film (Eastman Kodak).

MS Analysis of GFP-BD-CVIL–Derived Peptides

His$_6$-tagged GFP-BD-CVIL fusion protein expressed in *E. coli* was purified by Ni-affinity chromatography (i.e., with elution at 750 mM imidazole) and used as a standard. Transformed BY-2 cells expressing His$_6$-tagged GFP-BD-CVIL (165 mg fresh weight) were ground in liquid nitrogen and resuspended in buffer A consisting of 10 mM Tris-HCl, pH 8.0, 1 M NaCl, 20 mM glycerol, and 10 mM imidazole. The slurry was then incubated at room temperature for 30 min and centrifuged at 8000g for 30 min at 4°C. The supernatant was removed and stored on ice. The pellet was gently washed with buffer A and suspended in solubilization solution (1% n-dodecyl-β-ᴅ-maltopyranoside and 5 mM β-mercaptoethanol). After mechanical homogenization, incubation at room temperature for 30 min, and centrifugation at 8000g for 30 min at 4°C, aliquots of membrane extracts were subjected to semipreparative SDS-PAGE according to the Laemmli protocol (Laemmli, 1970). Collection of protein spots and in situ digestion were performed as described (Heintz et al., 2006). Briefly, after gel dehydration with acetonitrile, proteins were digested overnight at room temperature in 50 μL of a solution containing 12.5 ng μL^{-1} of a modified *Pseudomonas* endoproteinase Asp-N (Roche) prepared in 25 mM NH$_4$HCO$_3$. Finally, a double peptide extraction was performed, first with 50 μL of 60% (v/v) acetonitrile in 5% (v/v) formic acid, and subsequently with 95% (v/v) acetonitrile in 5% (v/v) formic acid. The samples were then vacuum-concentrated to 10 μL.

Peptide concentration and fractionation was performed on a solid-phase extraction microelution plate (HLB OASIS). The plate was placed on a manifold connected to a vacuum pump, and activation was performed with 200 μL of methanol. The plate was subsequently washed with 200 μL of water. A 10-μL portion of the peptide mixture was mixed with 90 μL of 0.5% formic acid and loaded into a vial. The peptides were then sequentially eluted in seven steps with 50 μL of 5, 10, 20, 35, 40, 60, and 95% methanol in 0.5% formic acid. The eluted fractions were vacuum-concentrated to 10 μL and subsequently used for MALDI-TOF MS and MS/MS analysis, which was performed on an Ultraflex TOF-TOF mass spectrometer (Bruker-Daltonik) as described elsewhere (Heintz et al., 2006). Theoretical masses (monoisotopic [M+H]$^+$ and average) for isoprenylated and methylated versus unprenylated peptides were calculated using BioTools v.3 software (Bruker-Daltonik).

Accession Number

Sequence data from this article can be found in the GenBank/EMBL data libraries under the following accession number: *O. sativa* CaM61, U37936.

Supplemental Data

The following materials are available in the online version of this article.

Supplemental Figure 1. MALDI-TOF/TOF MS/MS Spectra.

Supplemental Figure 2. Addition of Ca^{2+} or the Calmodulin Inhibitor Calmidazolium Does Not Affect the Localization of GFP-CaM61 or GFP-BD-CVIL.

Supplemental Figure 3. Mevinolin Treatment of BY-2 Cell Cultures Arrests Cell Growth.

Supplemental Table 1. χ^2 Analysis of Data in Figure 3.

Supplemental Table 2. χ^2 Analysis of Data in Figure 4.

REFERENCES

Adam, K.-P., Thiel, R., and Zapp, J. (1999). Incorporation of 1-[1-^{13}C] deoxy-D-xylulose in chamomile sequiterpenes. Arch. Biochem. Biophys. **369:** 127–132.

Alberts, A.W., et al. (1980). Mevinolin, a highly potent competitive inhibitor of hydroxymethylglutaryl-coenzyme A reductase and a cholesterol-lowering agent. Proc. Natl. Acad. Sci. USA **77:** 3957–3961.

Aoyama, T., and Chua, N.H. (1997). A glucocorticoid-mediated transcriptional induction system in transgenic plants. Plant J. **11:** 605–612.

Bach, T.J. (1995). Some new aspects of isoprenoid biosynthesis in plants - A review. Lipids **30:** 191–202.

Bach, T.J., and Lichtenthaler, H.K. (1983). Inhibition by mevinolin of plant growth, sterol formation and pigment accumulation. Physiol. Plant. **59:** 50–60.

Bick, J.A., and Lange, B.M. (2003). Metabolic cross talk between cytosolic and plastidial pathways of isoprenoid biosynthesis: Unidirectional transport of intermediates across the chloroplast envelope membrane. Arch. Biochem. Biophys. **415:** 146–154.

Bolte, S., Talbot, C., Boutte, Y., Catrice, O., Read, N.D., and Satiat-Jeunemaître, B. (2004). FM-dyes as experimental probes for dissecting vesicle trafficking in living plant cells. J. Microsc. **214:** 159–173.

Bonetta, D., Bayliss, P., Sun, S., Sage, T., and McCourt, P. (2000). Farnesylation is involved in meristem organization in Arabidopsis. Planta **211:** 182–190.

Boonburapong, B., and Buaboocha, T. (2007). Genome-wide identification and analyses of the rice calmodulin and related potential calcium sensor proteins. BMC Plant Biol. **7:** 4.

Bouvier, F., Rahier, A., and Camara, B. (2005). Biogenesis, molecular regulation and function of plant isoprenoids. Prog. Lipid Res. **44:** 357–429.

Burlat, V., Oudin, A., Courtois, M., Rideau, M., and St-Pierre, B. (2004). Co-expression of three MEP pathway genes and geraniol 10-hydroxylase in internal phloem parenchyma of *Catharanthus roseus* implicates multicellular translocation of intermediates during the biosynthesis of monoterpene indole alkaloids and isoprenoid-derived primary metabolites. Plant J. **38:** 131–141.

Caldelari, D., Sternberg, H., Rodríguez-Concepción, M., Gruissem, W., and Yalovsky, S. (2001). Efficient prenylation by a plant geranyl-geranyltransferase-I requires a functional CaaL box motif and a proximal polybasic domain. Plant Physiol. **126:** 1416–1429.

Cervantes-Cervantes, M., Gallagher, C.E., Zhu, C., and Wurtzel, E.T. (2006). Maize cDNAs expressed in endosperm encode functional farnesyl diphosphate synthase with geranylgeranyl diphosphate synthase activity. Plant Physiol. **141:** 220–231.

Clarke, S. (1992). Protein isoprenylation and methylation at carboxyl-terminal cysteine residues. Annu. Rev. Biochem. **61:** 355–386.

Criqui, M.C., Parmentier, Y., Derevier, A., Shen, W.H., Dong, A., and Genschik, P. (2000). Cell cycle-dependent proteolysis and ectopic overexpression of cyclin B1 in tobacco BY2 cells. Plant J. **6:** 763–773.

Crowell, D.N. (2000). Functional implications of protein isoprenylation in plants. Prog. Lipid Res. **39:** 393–408.

Cutler, S., Ghassemian, M., Bonetta, D., Cooney, S., and McCourt, P. (1996). A protein farnesyl transferase involved in abscisic acid signal transduction in Arabidopsis. Science **273:** 1239–1241.

Disch, A., Hemmerlin, A., Bach, T.J., and Rohmer, M. (1998). Mevalonate-derived isopentenyl diphosphate is the biosynthetic precursor of ubiquinone prenyl side chain in tobacco BY-2 cells. Biochem. J. **331:** 615–621.

Dong, A., Xin, H., Yu, Y., Sun, C., Cao, K., and Shen, W.-H. (2002). The subcellular localization of unusual rice calmodulin isoform OsCaM61 depends on its prenylation status. Plant Mol. Biol. **48:** 203–210.

Dudareva, N., Andersson, S., Orlova, I., Gatto, N., Reichelt, M., Rhodes, D., Boland, W., and Gershenzon, J. (2005). The non-mevalonate pathway supports both monoterpene and sesquiterpene formation in snapdragon flowers. Proc. Natl. Acad. Sci. USA **102:** 933–938.

Dykema, P.E., Sipes, P.R., Marie, A., Biermann, B.J., Crowell, D.N., and Randall, S.K. (1999). A new class of proteins capable of binding transition metals. Plant Mol. Biol. **41:** 139–150.

Eberhardt, N.L., and Rilling, H.C. (1975). Prenyltransferase from *Saccharomyces cerevisiae*. Purification to homogeneity and molecular properties. J. Biol. Chem. **250:** 863–866.

Eisenreich, W., Rohdich, F., and Bacher, A. (2001). Deoxyxylulosxe phosphate pathway to terpenoids. Trends Plant Sci. **6:** 78–84.

Eisenreich, W., Bacher, A., Arigoni, D., and Rohdich, F. (2004). Biosynthesis of isoprenoids via the non-mevalonate pathway. Cell. Mol. Life Sci. **61:** 1401–1426.

Galichet, A., and Gruissem, W. (2006). Developmentally controlled farnesylation modulates AtNAP1;1 function in cell proliferation and cell expansion during Arabidopsis leaf development. Plant Physiol. **142:** 1412–1426.

Gutiérrez-Nava, M.L., Gillmor, C.S., Jiménez, L.F., Guevara-García, A., and León, P. (2004). Chloroplast biogenesis genes act cell and noncell autonomously in early chloroplast development. Plant Physiol. **135:** 471–482.

Hartmann, M.-A., and Bach, T.J. (2001). Incorporation of all-*trans*-farnesol into sterols and ubiquinone in *Nicotiana tabacum* L. cv Bright Yellow-2 cell cultures. Tetrahedron Lett. **42:** 655–657.

Heintz, D., Erxleben, A., High, A.A., Wurtz, V., Reski, R., van Dorsselaer, A., and Sarnighausen, E. (2006). Rapid alteration of the phosphoproteome in the moss *Physcomitrella patens* after cytokinin treatment. J. Proteome Res. **5:** 2283–2293.

Hemmerlin, A., and Bach, T.J. (1998). Effects of mevinolin on cell cycle progression and viability of tobacco BY-2 cells. Plant J. **14:** 65–74.

Hemmerlin, A., and Bach, T.J. (2000). Farnesol-induced cell death and stimulation of 3-hydroxy-3-methylglutaryl-coenzyme A reductase activity in tobacco cv Bright Yellow-2 cells. Plant Physiol. **123:** 1257–1268.

Hemmerlin, A., Fischt, I., and Bach, T.J. (2000). Differential interaction of branch-specific inhibitors of isoprenoid biosynthesis with cell cycle progression in tobacco BY-2 cells. Physiol. Plant. **110:** 343–350.

Hemmerlin, A., Hoeffler, J.-F., Meyer, O., Tritsch, D., Kagan, I.A., Grosdemange-Billiard, C., Rohmer, M., and Bach, T.J. (2003). Cross-talk between the cytosolic mevalonate and the plastidial methylerythritol phosphate pathways in tobacco Bright Yellow 2 cells. J. Biol. Chem. **278:** 26666–26676.

Hemmerlin, A., Tritsch, D., Hartmann, M., Pacaud, K., Hoeffler, J.-F., van Dorsselaer, A., Rohmer, M., and Bach, T.J. (2006). A cytosolic Arabidopsis D-xylulose kinase catalyzes the phosphorylation of 1-deoxy-D-xylulose into a precursor of the plastidial isoprenoid pathway. Plant Physiol. **142:** 441–457.

Hoeffler, J.-F., Hemmerlin, A., Grosdemange-Billiard, C., Bach, T.J., and Rohmer, M. (2002). Isoprenoid biosynthesis in higher plants and in *Escherichia coli*: On the branching in the methylerythritol phosphate pathway and the independent biosynthesis of isopentenyl diphosphate and dimethylallyl diphosphate. Biochem. J. **366:** 573–583.

Johnson, C.D., Chary, S.N., Chernoff, E.A., Zeng, Q., Running, M.P., and Crowell, D.N. (2005). Protein geranylgeranyltransferase I is involved in specific aspects of abscisic acid and auxin signaling in Arabidopsis. Plant Physiol. **139:** 722–733.

Jux, A., Gleixner, G., and Boland, W. (2001). Classification of terpenoids according to the methylerythritolphosphate or the mevalonate pathway with natural $^{12}C/^{13}C$ isotope ratios: Dynamic allocation of resources in induced plants. Angew. Chem. Int. Ed. **40:** 2091–2093.

Kasahara, H., Hanada, A., Kuzuyama, T., Takagi, M., Kamiya, Y., and Yamaguchi, S. (2002). Contribution of the mevalonate and methylerythritol phosphate pathways to the biosynthesis of gibberellins in Arabidopsis. J. Biol. Chem. **277:** 45188–45194.

Kasahara, H., Takei, K., Ueda, N., Hishiyama, S., Yamaya, T., Kamiya, Y., Yamaguchi, S., and Sakakibara, H. (2004). Distinct isoprenoid origins of *cis*- and *trans*-zeatin biosyntheses in Arabidopsis. J. Biol. Chem. **279:** 14049–14054.

Kovacs, W.J., Olivier, L.M., and Krisans, S.K. (2002). Central role of peroxisomes in isoprenoid biosynthesis. Prog. Lipid Res. **41:** 369–391.

Kuntz, L., Tritsch, D., Grosdemange-Billiard, C., Hemmerlin, A., Willem, A., Bach, T.J., and Rohmer, M. (2005). Isoprenoid biosynthesis as a target for antibacterial and antiparasitic drugs: Phosphonohydroxamic acids as inhibitors of deoxyxylulose phosphate reductoisomerase. Biochem. J. **396:** 127–135.

Kuzuyama, T., and Seto, H. (2003). Diversity of the biosynthesis of the isoprene units. Nat. Prod. Rep. **20:** 171–183.

Laemmli, U.K. (1970). Cleavage of structural proteins during the assembly of the head of bacteriophage T4. Nature **227:** 680–685.

Lange, B.M., Ketchum, R.E., and Croteau, R. (2001). Isoprenoid biosynthesis. Metabolite profiling of peppermint oil gland secretory cells and application to herbicide target analysis. Plant Physiol. **127:** 305–314.

Laule, O., Fürholz, A., Chang, H.S., Zhu, T., Wang, X., Heifetz, P.B., Gruissem, W., and Lange, M. (2003). Crosstalk between cytosolic and plastidial pathways of isoprenoid biosynthesis in *Arabidopsis thaliana.* Proc. Natl. Acad. Sci. USA **100:** 6866–6871.

Lemichez, E., Wu, Y., Sanchez, J.P., Mettouchi, A., Mathur, J., and

Chua, N.H. (2001). Inactivation of AtRac1 by abscisic acid is essential for stomatal closure. Genes Dev. **15:** 1808–1816.

Li, H., Shen, J.J., Zheng, Z.L., Lin, Y., and Yang, Z. (2001). The Rop GTPase switch controls multiple developmental processes in Arabidopsis. Plant Physiol. **126:** 670–684.

Lichtenthaler, H.K. (2000). Non-mevalonate isoprenoid biosynthesis: Enzymes, genes and inhibitors. Biochem. Soc. Trans. **28:** 785–789.

Lichtenthaler, H.K., Zeidler, J., Schwender, J., and Müller, C. (2000). The non-mevalonate isoprenoid biosynthesis of plants as a test system for new herbicides and drugs against pathogenic bacteria and the malaria parasite. Z. Naturforsch. [C] **55:** 305–313.

Merret, R., Cirioni, J.-R., Bach, T.J., and Hemmerlin, A. (2007). A serine involved in actin-dependent subcellular localization of a stress-induced tobacco BY-2 hydroxymethylglutaryl-CoA reductase isoform. FEBS Lett. **581:** 5295–5299.

Miyazawa, Y., Kato, H., Muranaka, T., and Yoshida, S. (2002). Amyloplast formation in cultured tobacco BY-2 cells requires a high cytokinin content. Plant Cell Physiol. **43:** 1534–1541.

Müller, C., Schwender, J., Zeidler, J., and Lichtenthaler, H.K. (2000). Properties and inhibition of the first two enzymes of the non-mevalonate pathway of isoprenoid biosynthesis. Biochem. Soc. Trans. **28:** 792–793.

Nagata, T., Nemoto, Y., and Hasezawa, S. (1992). Tobacco BY-2 cell line as the "HeLa" cell in cell biology of higher plants. Int. Rev. Cytol. **132:** 1–30.

Okada, K., Saito, T., Nagakawa, T., Kawamukai, M., and Kamiya, Y. (2000). Five GGPPSs expressed in differrent organs are localized into three subcellular compartments in Arabidopsis. Plant Physiol. **122:** 1045–1056.

Okuhara, M., Kuroda, Y., Goto, T., Okamoto, M., Terano, H., Kohsaka, M., Aoki, H., and Imanaka, H. (1980). Studies on new phosphonic acid antibiotics. I. FR-900098, isolation and characterization. J. Antibiot. (Tokyo) **33:** 13–17.

Oudin, A., Mahrough, S., Courdavault, V., Hervouet, N., Zelwer, C., Rodriguez-Concepción, M., St-Pierre, B., and Burlat, V. (2007). Spatial distribution and hormonal regulatikon of gene products from methylerythritol phosphate and monoterpene-secoiridoid pathways in *Catharanthus roseus.* Plant Mol. Biol. **65:** 13–35.

Pei, Z.M., Ghassemian, M., Kwak, C.M., McCourt, P., and Schroeder, J.I. (1998). Role of farnesyltransferase in ABA regulation of guard cell anion channels and plant water loss. Science **282:** 287–290.

Piel, J., Donath, J., Bandemer, K., and Boland, W. (1998). Mevalonate-independent biosynthesis of terpenoid volatiles in plants: Induced and constitutive emission of volatiles. Angew. Chem. Int. Ed. **37:** 2478–2481.

Qian, D., Zhou, D., Ju, R., Cramer, C.L., and Yang, Z. (1996). Protein farnesyltransferase in plants: Molecular characterization and involvement in cell cycle control. Plant Cell **8:** 2381–2394.

Randall, S.K., Marshall, M.S., and Crowell, D.N. (1993). Protein isoprenylation in suspension-cultured tobacco cells. Plant Cell **5:** 433–442.

Rodríguez-Concepción, M. (2004). The MEP pathway: A new target for the development of herbicides, antibiotics and antimalarial drugs. Curr. Pharm. Des. **10:** 2391–2400.

Rodríguez-Concepción, M., and Boronat, A. (2002). Elucidation of the methylerythritol phosphate pathway for isoprenoid biosynthesis in bacteria and plastids. A metabolic milestone achieved through genomics. Plant Physiol. **130:** 1079–1089.

Rodríguez-Concepción, M., Yalovsky, S., Zik, M., Fromm, H., and Gruissem, W. (1999). The prenylation status of a novel plant calmodulin directs plasma membrane or nuclear localization of the protein. EMBO J. **18:** 1996–2007.

Rohmer, M. (1999). The discovery of a mevalonate-independent pathway for isoprenoid biosynthesis in bacteria, algae and higher plants. Nat. Prod. Rep. **16:** 565–574.

Rohmer, M., Grosdemange-Billiard, C., Seemann, M., and Tritsch, D. (2004). Isoprenoid biosynthesis as a novel target for antibacterial and antiparasitic drugs. Curr. Opin. Investig. Drugs **5:** 154–162.

Running, M.P., Fletcher, J.C., and Meyerowitz, E.M. (1998). The WIGGUM gene is required for proper regulation of floral meristem size in Arabidopsis. Development **125:** 2545–2553.

Running, M.P., Lavy, M., Sternberg, H., Galichet, A., Gruissem, W., Hake, S., Ori, N., and Yalovsky, S. (2004). Enlarged meristems and delayed growth in plp mutants result from lack of CaaX prenyltransferases. Proc. Natl. Acad. Sci. USA **101:** 7815–7820.

Sakakibara, H., Kasahara, H., Ueda, N., Kojima, M., Takei, K., Hishiyama, S., Asami, T., Okada, K., Kamiya, Y., Yamaya, T., and Yamaguchi, S. (2005). *Agrobacterium tumefaciens* increases cytokinin production in plastids by modifying the biosynthetic pathway in the host plant. Proc. Natl. Acad. Sci. USA **102:** 9972–9977.

Sandmann, G., and Böger, P. (1989). Inhibition of carotenoid biosynthesis by herbicides. In Target Sites of Herbicide Action, P. Böger and G. Sandmann, eds (Boca Raton, FL: CRC Press), pp. 25–44.

Schuhr, C.A., Radykewicz, T., Sagner, S., Latzel, C., Zenk, M.H., Arigoni, D., Bacher, A., Rohdich, F., and Eisenreich, W. (2003). Quantitative assessment of crosstalk between the two isoprenoid biosynthesis pathways in plants by NMR spectroscopy. Phytochem. Rev. **2:** 3–16.

Schwarz, M., and Arigoni, D. (1999). Ginkgolide biosynthesis. In Comprehensive Natural Product Chemistry, Vol. 2, D. Cane, ed (Oxford, UK: Pergamon), pp. 367–399.

Shipton, C.A., Parmryd, I., Swiezewska, E., Andersson, B., and Dallner, G. (1995). Isoprenylation of plant proteins in vivo. Isoprenylated proteins are abundant in the mitochondria and nuclei of spinach. J. Biol. Chem. **270:** 566–572.

Simonen, M., Ibig-Rehm, Y., Hofmann, G., Zimmermann, J., Albrecht, G., Magnier, M., Heidinger, V., and Gabriel, D. (2008). High-content assay to study protein prenylation. J. Biomol. Screen. **13:** 456–467.

Skorupinska-Tudek, K., et al. (2008). Contribution of the mevalonate and methylerythritol phosphate pathways to the biosynthesis of dolichols in plants. J. Biol. Chem. **283:** 21024–21035.

Suzuki, N., Yamaguchi, Y., Koizumi, N., and Sano, H. (2002). Functional characterization of a heavy metal binding protein Cdl19 from Arabidopsis. Plant J. **32:** 165–173.

Swiezewska, E., Thelin, A., Dallner, G., Andersson, B., and Ernster, L. (1993). Occurrence of prenylated proteins in plant cells. Biochem. Biophys. Res. Commun. **192:** 161–166.

Thai, L., Rush, J.S., Maul, J.E., Devarenne, T., Rodgers, D.L., Chappell, J., and Waechter, C.J. (1999). Farnesol is utilized for isoprenoid biosynthesis in plant cells via farnesyl pyrophosphate formed by successive monophosphorylation reactions. Proc. Natl. Acad. Sci. USA **96:** 13080–13085.

Trueblood, C.E., Ohya, Y., and Rine, J. (1993). Genetic evidence for in vivo cross-specificity of the CaaX-box protein prenyltransferases farnesyltransferase and geranylgeranyltransferase-I in *Saccharomyces cerevisiae.* Mol. Cell. Biol. **13:** 4260–4275.

Trusov, Y., Rookes, J.E., Tilbrook, K., Chakravorty, D., Mason, M.G., Anderson, D., Chen, J.-G., Jones, A.M., and Botella, J.R. (2007). Heterotrimeric G protein gamma subunits provide functional selectivity in G beta-gamma dimer signaling in Arabidopsis. Plant Cell **19:** 1235–1250.

Vasudevan, A., Qian, Y., Vogt, A., Blaskovich, M.A., Ohkanda, J., Sebti, S.M., and Hamilton, A.D. (1999). Potent, highly selective, and non-thiol inhibitors of protein geranylgeranyltransferase-1. J. Med. Chem. **42:** 1333–1340.

Yalovsky, S., Kulukian, A., Rodríguez-Concepción, M., Young, C.A., and Gruissem, W. (2000). Functional requirement of plant farnesyl-transferase during development in Arabidopsis. Plant Cell **12:** 1267–1278.

Yang, Z. (2002). Small GTPases: Versatile signaling switches in plants. Plant Cell **14**(Suppl): S375–S388.

Xiao, C., Xin, H., Dong, A., Sun, C., and Cao, K. (1999). A novel calmodulin-like protein gene in rice which has an unusual prolonged C-terminal sequence carrying a putative prenylation site. DNA Res. **6:** 179–181.

Zeidler, J., Schwender, J., Müller, C., and Lichtenthaler, H.K. (2000). The non-mevalonate isoprenoid biosynthesis of plants as a test system for drugs against malaria and pathogenic bacteria. Biochem. Soc. Trans. **28:** 796–798.

Zhang, F.L., and Casey, P.J. (1996). Protein prenylation: Molecular mechanisms and functional consequences. Annu. Rev. Biochem. **65:** 241–269.

Zhu, J.K., Bressan, R.A., and Hasegawa, P.M. (1993). Isoprenylation of the plant molecular chaperone ANJ1 facilitates membrane association and function at high temperature. Proc. Natl. Acad. Sci. USA **90:** 8557–8561.

Ziegelhoffer, E.C., Medrano, L.J., and Meyerowitz, E.M. (2000). Cloning of the Arabidopsis WIGGUM gene identifies a role for farnesylation in meristem development. Proc. Natl. Acad. Sci. USA **97:** 7633–7638.